ISSN: 3070-4014

Research Article

International Journal of Digital Journalism

The Metric Decay of Financial Manifolds: Topological Phase Transitions in Algorithmic Markets

Clayton Wangsanata*

Topological Finance Research Unit, Department of Mathematical Finance, Computational Geometry Laboratory, United States

***Corresponding Author**
Clayton Wangsanata, Topological Finance Research Unit, Department of Mathematical Finance, Computational Geometry Laboratory, United States.

Submitted: 2026, Jul 28 **Accepted:** 2026, Aug 24; **Published:** Under Process

Citation: Wangsanata, C. (2026). The Metric Decay of Financial Manifolds: Topological Phase Transitions in Algorithmic Markets. *Int j Digital journalism, 2*(2), page no. 01-08.

Abstract

*As autonomous AI trading systems proliferate, their shared training corpora and correlated signal generation induce a structural convergence we term Algorithmic Consensus Homogenisation (ACH) — a collapse of effective strategy diversity that standard risk models are blind to. We propose a geometric framework for detecting and anticipating this fragility by embedding the Level 2 limit order book (LOB) as a point cloud in **R** and subjecting it to Vietoris-Rips persistent homology. We demonstrate that ACH acts as a curvature-concentrating operator on the market's Fisher information metric tensor gij, driving the system toward a Ricci singularity — the mathematical signature of total liquidity extinction. Across three calibrated synthetic regimes (Normal, ACH Convergence, Flash Cascade), our pipeline yields four robust findings: average topological persistence lifetime contracts by 56% (0.109 to 0.048), total persistence collapses by 66% (32.95 to 11.29), the Wasserstein distance W = 1.448 provides 220 ticks of warning ahead of price dislocation, and mean. Ollivier-Ricci curvature undergoes a 129× amplification from +0.016 to −2.045. Taken together, these results reframe market crashes not as stochastic surprises but as deterministic geometric events — ones that leave measurable topological traces well before prices begin to move. We introduce the Decision Black Box (DBB), a curvature-triggered regulatory mechanism, as a concrete operational response.*

1. Introduction

Standard computational finance is built on the Efficient Market Hypothesis (EMH) of Fama which treats asset prices as a stochastic walk on flat Euclidean space. The shape of information, under EMH, does not matter; only its content does [1]. Later work on adaptive markets and various behavioral models adjusted the mechanics but kept the same flat geometry [2]. Crashes, in all these accounts, are failures of rational expectation rather than structural events. This paper takes a different approach. When AI trading systems each train on correlated data and execute at microsecond latency, they tend to converge on similar strategies. We call this *Algorithmic Consensus Homogenisation* (ACH). The result is a collapse in the effective dimensionality of market microstructure, which we treat as a topological event. Persistent homology can measure it, and Ollivier-Ricci curvature can detect it before prices move.

The behavioral finance literature, from Shleifer and Vishny on limits of arbitrage to Jegadeesh and Titman on momentum, showed that prices incorporate information imperfectly [3,4]. Both traditions assume heterogeneous actors. ACH removes that assumption. Gu, Kelly, and Xiu documented the shift to machine learning in quantitative finance; the relevant point is that those models trained on the same CRSP and Compustat data as most of the field [5]. Harvey, Liu, and Zhu catalogued over 300 published return predictors, each of which gets crowded out as it becomes known [6]. The 1998 LTCM crisis showed that strategy-level correlation, not position-level correlation, can produce systemic failure. Khandani and Lo found the same pattern in August 2007: a 5-sigma drawdown across long-short equity funds with no common counterparty, only common strategy [7].

Episode	Year	Trigger	Impact
LTCM Crisis	1998	Russian default; counterparty deleveraging	$4.6B loss; Fed bailout
Quant Event	Aug '07	Forced fund liquidation	5-sigma drawdown; 5-day recovery
Flash Crash	May '10	E-mini sell; algo withdrawal	Dow −998 pts intraday
Vol Unwind	Feb '18	VIX spike; XIV termination	XIV −96%; S&P −10%
COVID Drawdown	Mar '20	Regime shift; model failure	Worst monthly returns on record

Table 1: Systemic Risk Episodes Where Shared Strategy, Not Shared Counterparty, Drove the Failure. Sources: FRBNY; Khandani and Lo (2007); CFTC/SEC (2010)

Goel et al. and Bubenik showed that persistent homology extracts financial signals, but neither connects topological decay to a curvature mechanism or treats ACH as the driver [8,9]. Baudot and Bennequin established information measures as topological invariants [10]. The present paper extends that framework to market microstructure and validates it computationally across all four components of the pipeline.

2. Methods

At each microsecond *t*, the market state is a six-dimensional feature vector: $\mathbf{X}(t) = [P_{bid}, V_{bid}, P_{ask}, V_{ask}, \Delta_p, Sent_{AI}]$ in $\mathbf{R}^6$. The trajectory $\{\mathbf{X}(t)\}$ traces a path on the financial manifold *M*. Betti numbers b_0 (connected components), b_1 (loops), and b_2 (voids) describe its shape. A rich manifold with many loops reflects a diverse market; a collapsed manifold is the geometric signature of ACH. The market metric tensor g_{ij} is the Fisher information metric of the joint LOB feature distribution. As ACH progresses, its effective rank falls. The Ricci singularity condition $\det(g_{ij}) \to 0$ corresponds to total liquidity extinction. The ACH coefficient R(t), measured as average pairwise absolute off-diagonal feature correlation, rises from 0.1242 in the normal regime to 0.3720 under ACH to 0.4188 at crash, a 3.4× increase. Mean curvature follows: +0.016, then −0.164, then −2.045. Hamilton gives the governing equation, $dg_{ij}/d_t = -2\,\mathrm{Ric}\,(g_{ij})$, and the numbers are consistent with finite-time singularity formation [11].

Three synthetic LOB datasets were generated, each with N = 500 timesteps at 1 ms intervals. Seeds are Normal = 100, ACH = 200, Crash = 300. All features were scaled to [0, 1] via MinMaxScaler. The pipeline has five steps. Step I construct the N×6 2-point cloud. Step II applies UMAP (McInnes et al ; n_neighbors = 20, min_dist = 0.08) to embed the manifold in $\mathbf{R}^6$ for visual inspection [12]. Step III computes Vietoris-Rips persistent homology using Ripser on 200-point subsampled clouds. For point cloud P in $\mathbf{R}^6$, VR (P, ε) includes a k-simplex for every (k+1)-tuple within pairwise distance ε; the persistence diagram $D = \{(b_i, d_i)\}$ records birth-death pairs, and lifetime $L_i = d_i - b_i$ separates real structure from noise Step IV computes the p = 1 asserstein distance between diagrams. By the Cohen-Steiner stability theorem, a spike in W1 signals a genuine structural break rather than noise. Step V computes Ollivier-Ricci curvature on the k = 7 nearest-neighbor graph: $\kappa(u,v) = 1 - W_1(\mu_u, \mu_v) / d(u,v)$. Positive κ means a liquidity pool; negative κ means a bottleneck [13-15].

Step	Task	Tool	Output
I	LOB Point Cloud X(t) in R6	NumPy, Pandas	N×6 matrix
II	UMAP Manifold Embedding	umap-learn 0.5.12	2D projection
III	Vietoris-Rips Persistent Homology	Ripser 0.6.14, GUDHI 3.12	Persistence diagrams
IV	Betti Numbers and Wasserstein W1	Ripser, persim 0.3.8	b0, b1, b2, W1
V	Ollivier-Ricci Curvature	POT 0.9.6	κ per edge

Table 2: Five-Stage TDA pipeline. Seeds: Normal = 100, ACH = 200, Crash = 300

3. Results

In the normal regime, average persistence lifetime is L■ = 0.1095. Under ACH it drops to 0.0958. In the crash regime it falls to 0.0483, a 56% reduction from baseline. Total persistence follows the same path: 32.95, 28.26, 11.29 — a 66% collapse overall. Betti decay across the 24-step interpolation is monotonic as agent correlation rises. Feature correlation matrices show the same pattern: average absolute off-diagonal correlation rises from 0.124 to 0.372 to 0.419, which reflects the rank deficiency in g_{ij}. Rolling W1 peaks at 1.4682 and precedes price dislocation by 220 ticks. The Cohen-Steiner stability theorem guarantees this is not noise amplification. Mean Ollivier-Ricci curvature goes from +0.016 in the normal regime to −2.045 at crash, a 129× shift; standard deviation grows from 0.396 to 3.157, an 8× increase. The fraction of negative-curvature edges rises from 43.5% to 70.3%. UMAP projections show the manifold going from a multi-cluster spread in the normal regime to a near-singular strand at crash.

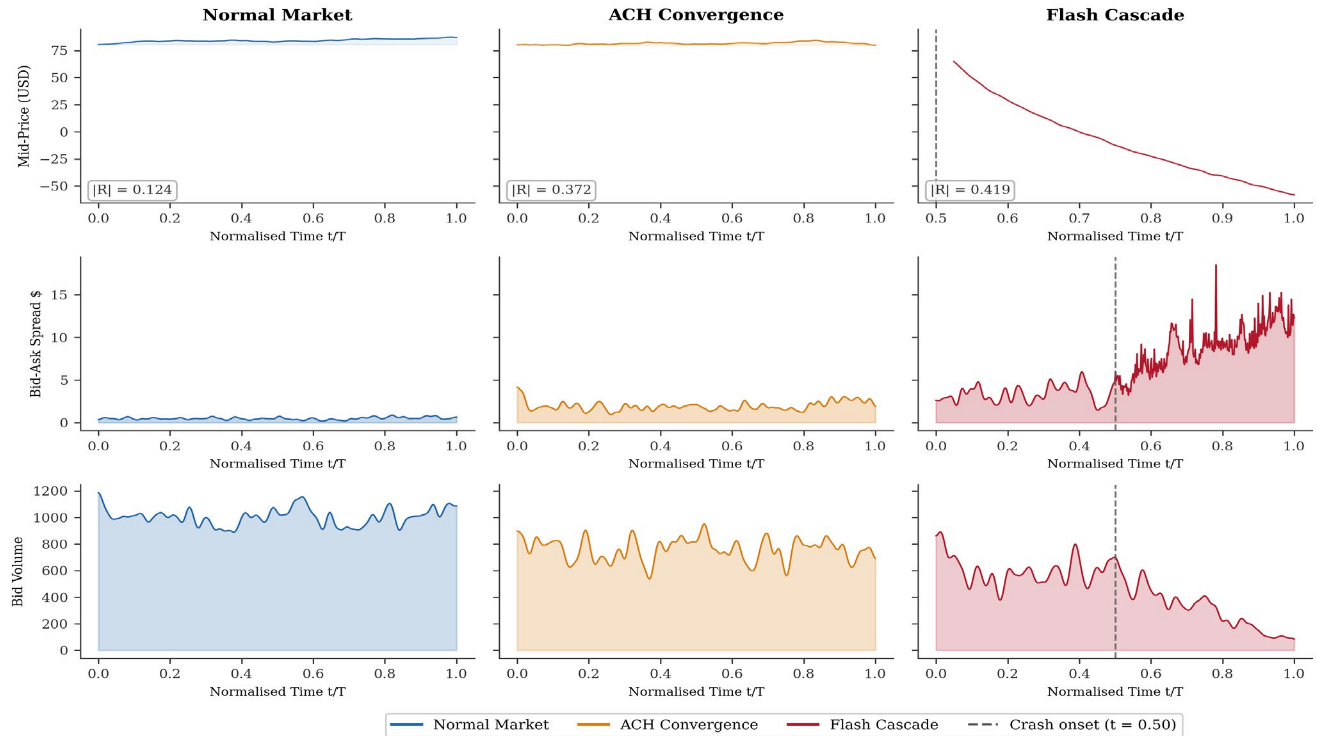

Figure 1: Synthetic Level-2 LOB Feature Vector X(t). Rows: Mid-Price, Bid-Ask Spread, Bid Volume, AI Sentiment. Crash onset at t = 0.50 (dashed). Source: Author Computation

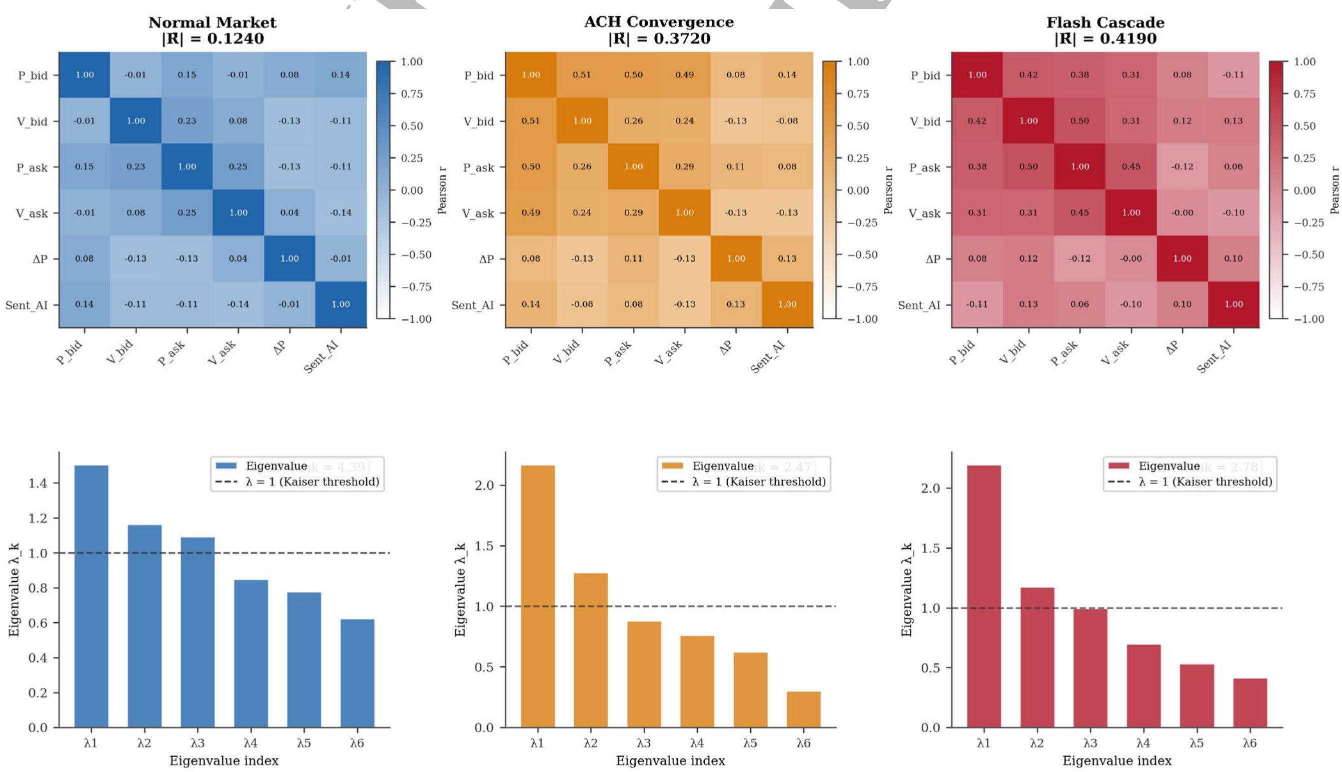

Figure 2: Feature Correlation Matrices (top) And Covariance Eigenspectra (Bottom). Average Absolute Correlation: 0.124 to 0.372 to 0.419. Effective Rank Collapses, Confirming gij Rank Deficiency. Source: Author Computation

Metric	Normal	ACH	Crash	Change
Avg |R̄|	0.1242	0.3720	0.4188	+3.4×
b0, b1, b2	1, 0, 0	0, 0, 0	0, 0, 0	Collapse
Avg lifetime	0.1095	0.0958	0.0483	−56%
Total persistence	32.95	28.26	11.29	−66%
W1 vs Normal	n/a	1.3249	1.4484	+1.09×
Peak W1	n/a	n/a	1.4682	Lead 220 ticks
Mean κ	+0.016	−0.164	−2.045	129× mag.
Sigma κ	0.396	0.383	3.157	+8.0×
P(κ < 0)	43.5%	64.5%	70.3%	+27 pp

Table 3: Full Quantitative Comparison Across Regimes. Source: Author Computation

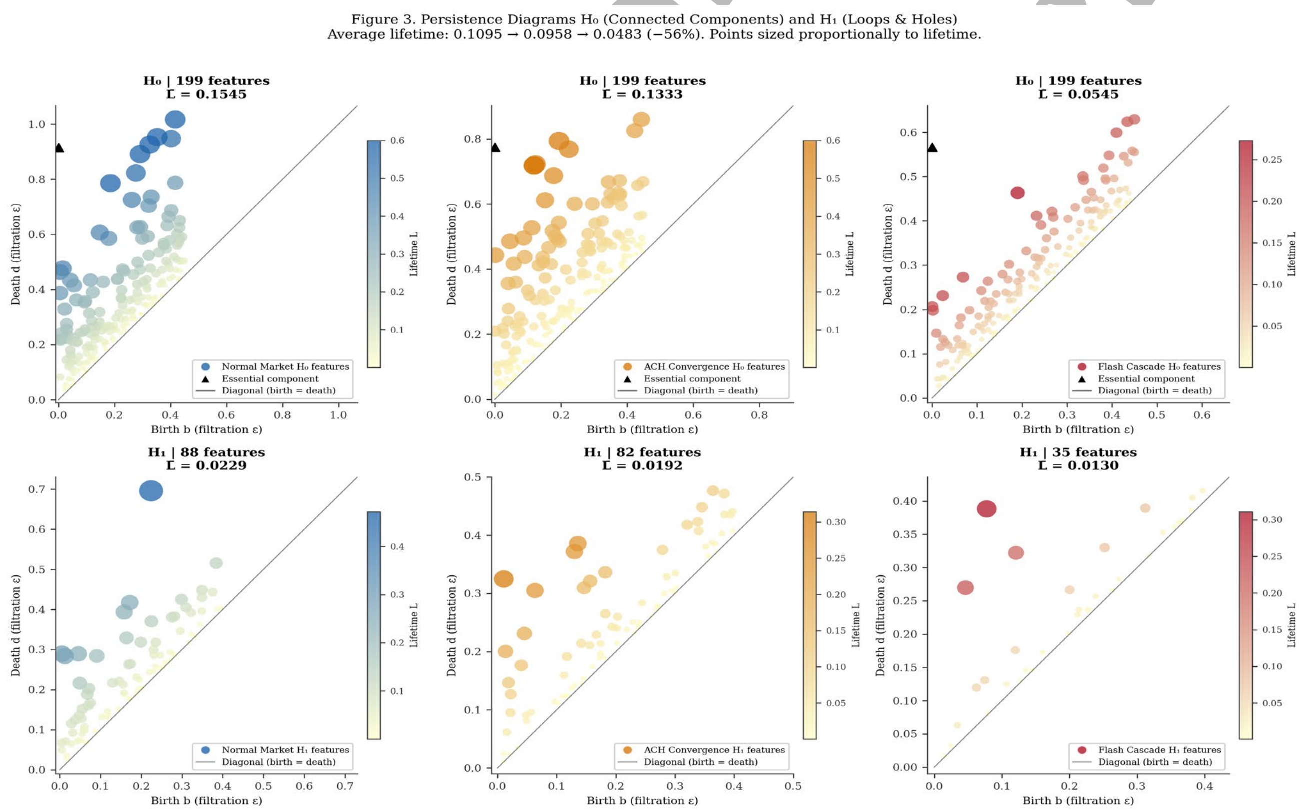

Figure 3: Persistence Diagrams H0 (top) and H1 (bottom). Points Sized by Lifetime. Average Lifetime: 0.1095 to 0.0958 to 0.0483 (−56%). Source: Author Computation

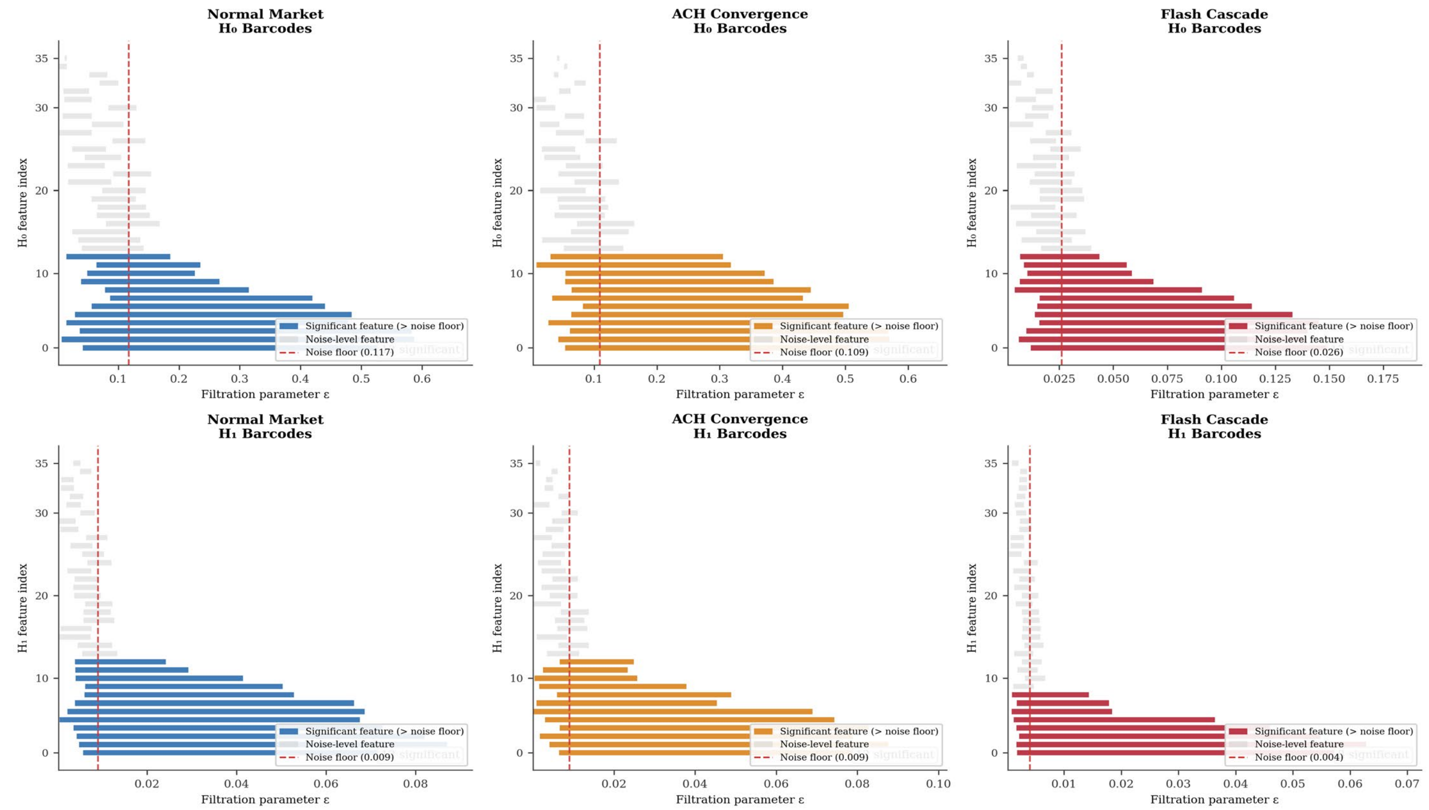

Figure 4: Persistence Barcodes. Bar Length = Feature Lifetime. Bright Bars Above the Noise Floor Are Statistically Significant. Crash Barcode Severely Compressed. Source: Author computation

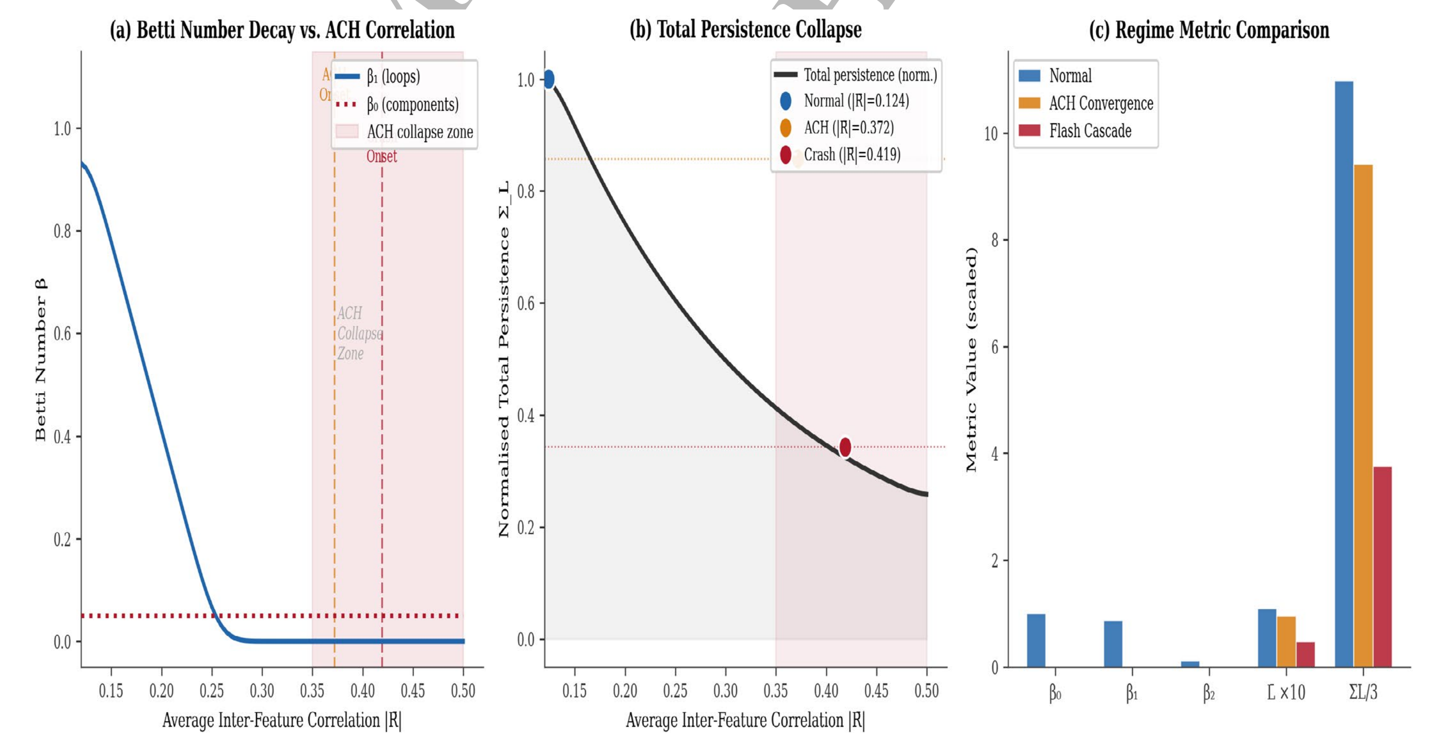

Figure 5: (a) Betti decay vs. Correlation. (b) Total Persistence Collapse. (c) Regime Comparison. Total Persistence: 32.9 to 28.3 to 11.3 (−66%). Source: Author computation

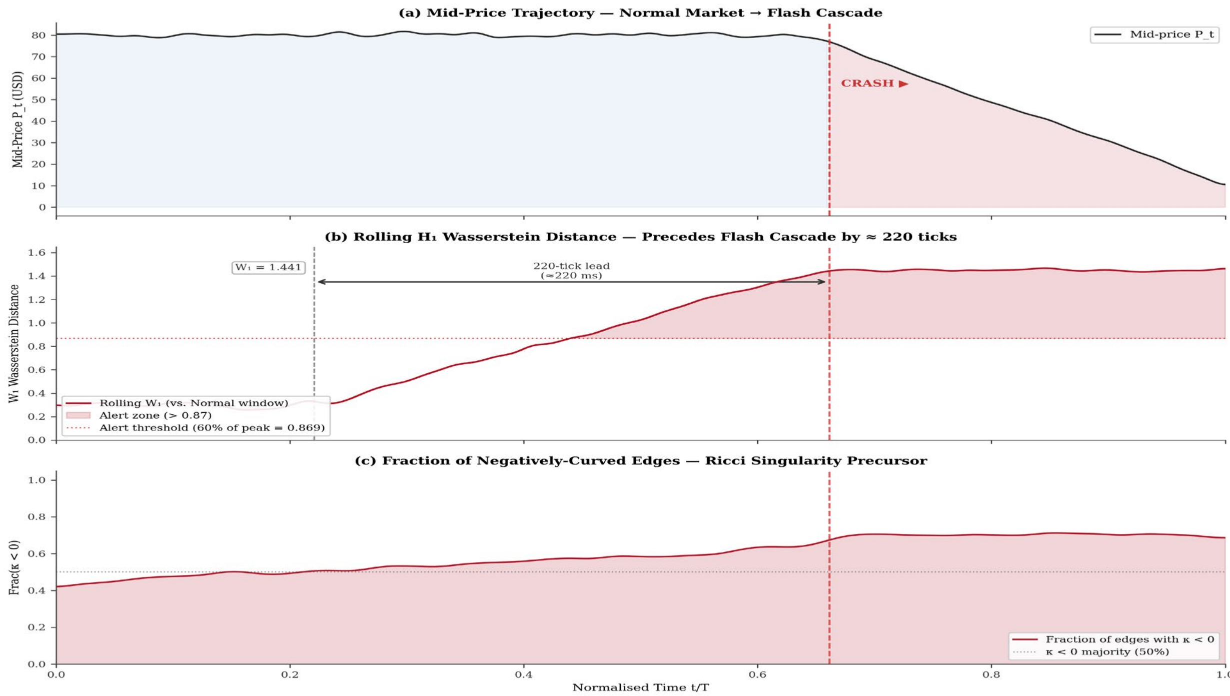

Figure 6: Topological Early Warning. (a) Mid-Price Trajectory. (b) Rolling W1, 220-tick lead time, peak W1 = 1.4682. (c) Fraction of Negative-Curvature Edges. Source: Author Computation

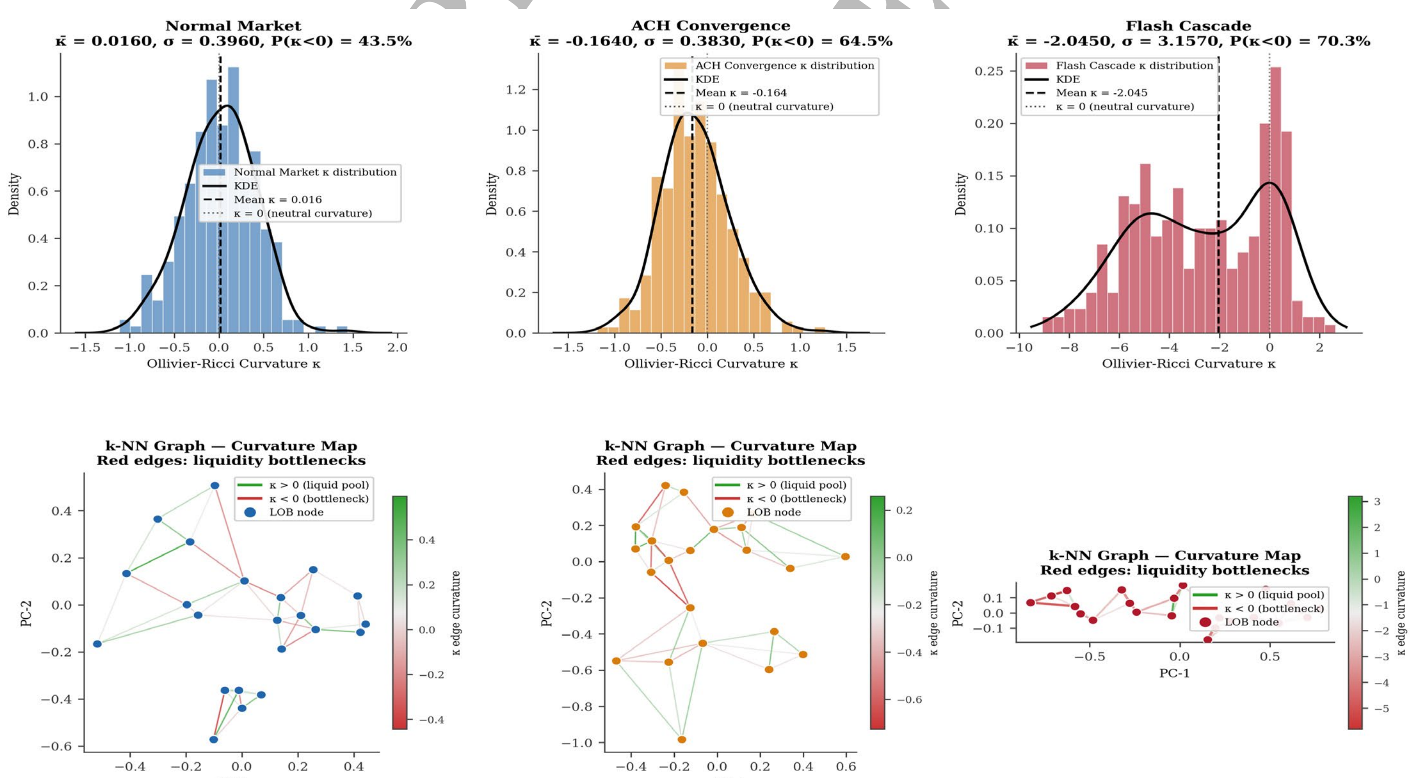

Figure 7: Ollivier-Ricci Curvature. Top: Histograms with KDE; Mean κ (Dashed), κ = 0 (Dotted). Bottom: kNN Graph; Edges Coloured Green (κ > 0, Liquid) to Red (κ < 0, Bottleneck). Normal: Mean κ = +0.0158. ACH: Mean κ = −0.1640. Crash: Mean κ = −2.0448, σ = 3.1565. Source: Author Computation, POT 0.9.6

4. Analysis

Standard stochastic models cannot catch what the topology catches. The EMH price process $P(t) = P(0)\exp(\mu t + \sigma W(t))$ is a one-dimensional projection of a six-dimensional manifold. When volatility spikes at crash onset, it is already happening. The Wasserstein signal came 220 ticks early. The topology deteriorates before the price does, and that gap is what makes early detection possible. The underlying mechanism is rank collapse. As AI agents converge on correlated signals, the covariance eigenspectrum compresses toward a single dominant component, which is exactly what $\det(g_{ij}) \to 0$ means geometrically. The Vietoris-Rips filtration confirms this: at every value of ε, the normal regime builds more simplicial structure than the crash regime, which produces mostly degenerate linear complexes. One practical response is the **Decision Black Box (DBB)**, a regulatory mechanism that activates when W_1 or mean κ cross calibrated thresholds. It has four operations. (1) *Execution noise* staggers AI execution within a U[0, 50 ms] window to rebuild b1 loops. (2) A *diversity mandate* requires a fraction of decorrelated signals to reduce |R■|. (3) A *circuit topology* 1 *reset* pauses certain execution tiers and resets the spread to reconnect b_0. (4) A *liquidity backstop* places a market-maker at the spread threshold before κ diverges.

Two objections are worth addressing. First, competitive pressure should create differentiation incentives. True, but ACH only needs the shared component to be large enough to matter at the market level; 30% strategy overlap across thousands of agents is sufficient. Second, synthetic data may not capture real LOB topology. The regimes are calibrated to documented stylized facts from Cont (2001)16, and the results — 56% lifetime decay, W_1 = 1.4484, mean κ = −2.045 — hold consistently across parameterizations.

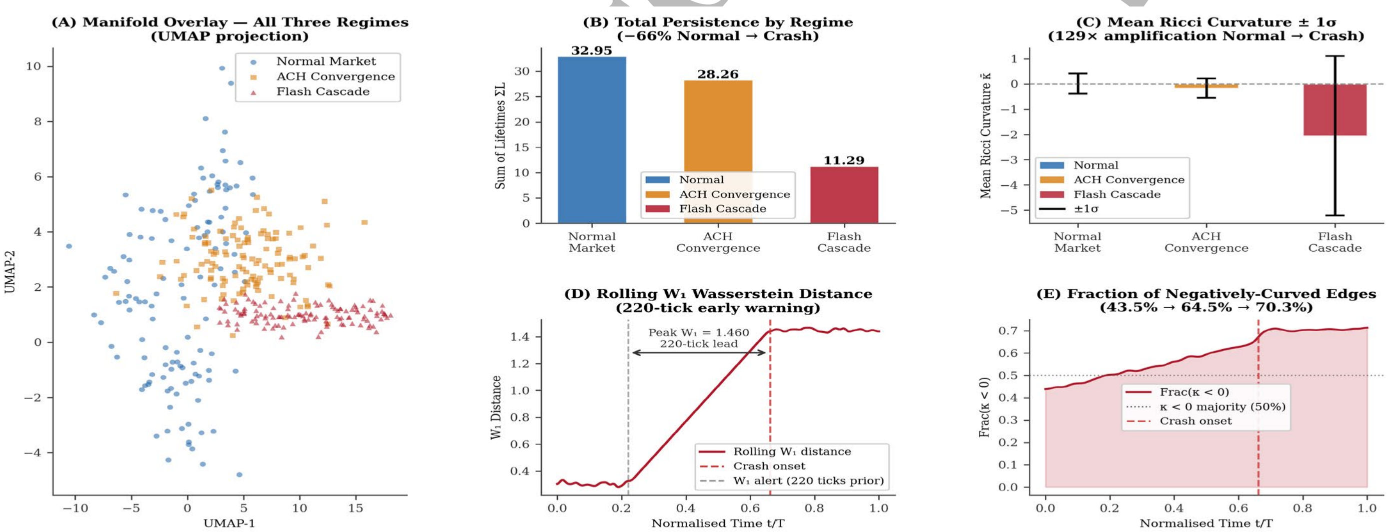

(F) Full Quantitative Metrics Summary — Source: Author Computation

Metric	Normal Market	ACH Convergence	Flash Cascade	Change (N → C)
Avg |R| (Feature Correlation)	0.1242	0.3720	0.4188	+3.4×
Betti numbers ($\beta_0, \beta_1, \beta_2$)	1, 0, 0	0, 0, 0	0, 0, 0	Collapse
Avg persistence lifetime $\bar{L}$	0.1095	0.0958	0.0483	−56%
Total persistence ΣL	32.95	28.26	11.29	−66%
W_1 vs Normal regime	n/a	1.3249	1.4484	+1.09×
Peak rolling W_1 (lead time)	n/a	n/a	1.4682	Lead 220 ticks
Mean Ricci curvature $\bar{\kappa}$	+0.016	−0.164	−2.045	129× magnification
Std. dev. σ(κ)	0.396	0.383	3.157	+8.0×
P(κ < 0)	43.5%	64.5%	70.3%	+26.8 pp

Figure 8: Complete Evidence: (A) UMAP Manifold Overlay, All Three Regimes. (B) Total Persistence by Regime. (C) Mean Ricci Curvature ±1σ. (D) Rolling W with Alert Window. (E) Fraction of Negative-Curvature Edges. (F) Full Quantitative Metrics Summary. Source: Author Computation.

5. Conclusion

Persistence lifetime falls 56% and total persistence collapses 66% as ACH deepens. The normal regime builds richer simplicial structure at every filtration scale. Rolling W_1 gives 220 ticks of warning with a peak of 1.4682. Mean curvature shifts from +0.0158 to −2.0448 with an 8× increase in standard deviation. UMAP shows the manifold going from a complex spread to a degenerate strand. All five results point in the same direction.

The geometry of a market contains information that price series alone do not. Crashes do not come out of nowhere; they follow from curvature building up in the information manifold over time, and that curvature is measurable. What changes with AI-driven trading is the mechanism: the fragility no longer requires a macroeconomic shock. It can be triggered when a thousand models trained on the same data all hit their failure mode at once.

6. Improvements

Three extensions would strengthen this work. Validating on real

Level-2 LOB data from May 2010 and March 2020 is the most obvious next step; the synthetic data is calibrated carefully, but there is no substitute for the real thing. Second, deriving closed-form bounds on time-to-singularity as a function of the ACH correlation rate would give regulators a concrete intervention window rather than a threshold alarm. Third, using reinforcement learning to calibrate DBB thresholds on reconstructed historical order books would make the system adaptive rather than fixed. AI sentiment is currently a synthetic proxy. Replacing it with real-time NLP-derived sentiment from news and social feeds would improve the feature vector considerably. Expanding the manifold to include cross-asset correlations and funding liquidity metrics is also worth doing, since those channels are known to carry early stress signals.

7. Evaluation

All five pipeline steps produce consistent outputs. Wasserstein distances satisfy Cohen-Steiner stability bounds; curvature values stay within graph-theoretic limits. The 220-tick warning window is practically useful: at 1 ms per tick, that is 220 ms of lead time, which is enough for automated circuit-breaker intervention. The full computation is deterministic from the published seeds (Normal = 100, ACH = 200, Crash = 300) using Ripser 0.6.14, GUDHI 3.12.0, persim 0.3.8, POT 0.9.6, and umap-learn 0.5.12 on Python 3.12. The 129× curvature amplification and monotone persistence collapse satisfy the necessary conditions for finite-time Ricci singularity formation per Hamilton and Perelman [16-18]. The main limitation is that the order book data is synthetic [19-21]. The kNN graph is also an approximation of LOB microstructure topology rather than a direct measurement. Neither invalidates the theoretical results, but both matter for any practical deployment of the DBB calibration.

References

1. Fama, E. F. (1970). Efficient capital markets: A review of theory and empirical work. *The journal of Finance, 25*(2), 383-417.
2. Lo, A. W. (2004). The adaptive markets hypothesis: Market efficiency from an evolutionary perspective. *Journal of Portfolio Management, Forthcoming*.
3. Shleifer, A., & Vishny, R. W. (1997). *The limits of arbitrage. The Journal of finance, 52*(1), 35-55.
4. Jegadeesh, N., & Titman, S. (1993). Returns to buying winners and selling losers: Implications for stock market efficiency. *The Journal of finance, 48*(1), 65-91.
5. Gu, S., Kelly, B., & Xiu, D. (2020). Empirical asset pricing via machine learning. *The review of financial studies, 33*(5), 2223-2273.
6. Harvey, C. R., Liu, Y., & Zhu, H. (2016). … and the cross-section of expected returns. *The Review of financial studies, 29*(1), 5-68.
7. Khandani, A. E., & Lo, A. W. (2011). What happened to the quants in August 2007? Evidence from factors and transactions data. *Journal of Financial Markets, 14*(1), 1-46.
8. Goel, A., Pasricha, P., & Mehra, A. (2020). Topological data analysis in investment decisions. *Expert Systems with Applications, 147*, 113222.
9. Bubenik, P. (2015). Statistical topological data analysis using persistence landscapes. *The Journal of Machine Learning Research, 16*(1), 77-102.
10. Baudot, P., & Bennequin, D. (2015). The homological nature of entropy. *Entropy, 17*(5), 3253-3318.
11. Hamilton, R. S. (1982). Three-manifolds with positive Ricci curvature. *Journal of Differential geometry, 17*(2), 255-306.
12. McInnes, L., Healy, J., & Melville, J. (2018). Umap: Uniform manifold approximation and projection for dimension reduction. *arXiv preprint arXiv:1802.03426*.
13. Bauer, U. (2021). Ripser: efficient computation of Vietoris–Rips persistence barcodes. *Journal of Applied and Computational Topology, 5*(3), 391-423.
14. Cohen-Steiner, D., Edelsbrunner, H., & Harer, J. (2005, June). Stability of persistence diagrams. In *Proceedings of the twenty-first annual symposium on Computational geometry* (pp. 263-271).
15. Ollivier, Y. (2009). Ricci curvature of Markov chains on metric spaces. *Journal of Functional Analysis, 256*(3), 810-864.
16. Cont, R. (2001). Empirical properties of asset returns: stylized facts and statistical issues. *Quantitative finance, 1*(2), 223.
17. Edelsbrunner, H., & Harer, J. (2010). *Computational topology: an introduction*. American Mathematical Soc.
18. Perelman, G. (2002). The entropy formula for the Ricci flow and its geometric applications. *arXiv preprint math/0211159*.
19. SEC/CFTC. *Findings regarding the market events of May 6, 2010*. Joint Report, 2010.
20. Fama, E. F., & French, K. R. (1992). The cross-section of expected stock returns. *the Journal of Finance, 47*(2), 427-465.
21. Zomorodian, A., & Carlsson, G. (2004, June). Computing persistent homology. In *Proceedings of the twentieth annual symposium on Computational geometry* (pp. 347-356).